PHYSICAL REVIEW D VOLUME 21, NUMBER 1 1 JANUARY 1980

# Photoproduction of large-transverse-momentum hadronic jets

J. F. Owens
*Physics Department, Florida State University, Tallahassee, Florida 32306*
(Received 6 August 1979; revised manuscript received 27 December 1979)

High-$p_T$ jet photoproduction can serve as a source of new information not obtainable with hadron beams alone. The pointlike nature of the photon-quark interaction gives rise to a new class of hard-scattering subprocesses so that the high-$p_T$ events will consist of both three- and four-jet topologies. The separation of these two contributions, which can be done on a purely kinematic basis, leads to new tests of the underlying dynamics. Further, by using quantum chromodynamics it is possible to calculate the parton distribution functions of the photon without any phenomenological input parametrizations. This fact can be exploited in the development of techniques for enhancing the fraction of quark-jet or gluon-jet triggers which, in turn, may be of use in searching for differences between quark and gluon jets. Detailed cross-section predictions together with estimates of backgrounds and sources of theoretical uncertainty are presented.

## I. INTRODUCTION

With the advent of quantum chromodynamics (QCD) and its property of asymptotic freedom, the study of large-momentum-transfer phenomena has assumed new importance in the study of the interactions of the hadron constituents.[1,2] High-$p_T$ particle[3] and jet production[4] have both made significant contributions to this endeavor. Experiments with proton and pion beams have already yielded new information on the underlying hard-scattering subprocesses[4] and also on the parton distribution functions of the incoming hadrons.[5] It is the purpose of this paper to point out the advantages of augmenting these existing studies with experiments performed with photon beams.

The unique feature of the photon, as compared to hadrons, is its pointlike coupling to quarks. As a result of this, high-energy photons will interact with partons in the target hadron to give two distinctly different types of high-$p_T$ event topologies. The pointlike interaction results in events for which there are no beam fragments. These events then have a characteristic three-jet structure—one jet of low-$p_T$ target fragments and two high-$p_T$ jets. The photon can also serve as a source of quarks and gluons and the distribution functions of these partons can be calculated in QCD with no additional input beyond the strong-interaction scale parameter $\Lambda$. Thus, the usual parton-parton hard-scattering subprocesses which contribute to the high-$p_T$ hadron-hadron cross section will appear here as well. These events have the characteristic four-jet structure since there will be fragments coming from the beam which will appear as a second low-$p_T$ jet. In the three-jet events all of the photon energy contributes to the hard-scattering subprocesses whereas only a fraction of it contributes to the four-jet topology. The resulting kinematic differences make it possible to separate these two event classes with a properly designed detector. This feature, when combined with the QCD-predicted parton distributions of the photon, makes it possible to identify kinematic regions which should give rise to an enhanced number of gluon-jet or quark-jet triggers. By comparing the jet structures observed in these different regions it should be possible to deduce information concerning the differences between quark and gluon jets.

The distributions of partons in hadrons fall as $(1-x)^n$ as $x$ goes to 1, where $x$ is the parton momentum fraction. Typically, for valence quarks $n=1$ (3) for pions (nucleons) and the powers are higher for gluons and sea quarks. For photons, however, the quark distributions are much harder, i.e., flatter in $x$. This means that in the four-jet events more of the photon's energy is available to the hard-scattering subprocess than in the purely hadronic case. Of course, in the three-jet events all of the photon's energy is available. Therefore, photon beams are more efficient than hadron beams at producing high-$p_T$ events. At sufficiently large $p_T$ the cross-section ratio is not suppressed as much as might be expected for an electromagnetic process. These larger cross sections mean that the high-$p_T$ jet measurements proposed here are in fact practical and may be undertaken with the existing photon beams at Fermilab and CERN.

The plan of the paper is as follows. In Sec. II the necessary theoretical input is presented. Included here is a short review of the photon parton-distribution-function calculation. In Sec. III the QCD perturbation-theory predictions are presented for a variety of observables using both single- and double-arm triggers. Section IV is devoted to a discussion of possible backgrounds and other complications not included in the predictions of

 

Sec. III. A summary and some conclusions are presented in Sec. V.

## II. THEORETICAL INPUT

### A. Parton distribution functions

Calculations of the structure function of the photon have been presented by a number of authors. Various techniques have been employed such as the operator-product expansion,[6] diagrammatic methods,[7] and a generalization[8] of the integrodifferential equation approach of Altarelli and Parisi.[9] All three approaches are physically equivalent and, indeed, agreement is found for the quark distributions in a photon. However, for the gluon distribution a discrepancy exists. The result given in Ref. 8 is too small by a factor of 3 for the gluon distribution, summed over all colors, while the correct result is given in Ref. 7 (for the case of a single color). For this reason a short review of the photon parton-distribution-function calculation will be given here.

Of the three techniques listed above, the derivation is simplest using the generalization of the Altarelli-Parisi equations as given in Ref. 8. The derivation proceeds exactly as in the nucleon case with parton distribution functions $G_{i/\gamma}(x, Q^2)$ and functions $P_{ij}(x)$ which are defined so that the probability of finding a parton $i$ in a parton $j$ with momentum fraction $x$ at a length scale between $t$ and $t+dt$ is just given by

$$\frac{\alpha_s(t)}{2\pi} P_{ij}(x)dx dt , \tag{1}$$

where $\alpha_s(t)$ is the strong running coupling constant given by $\alpha_s(t)=1/bt$ with $b=(33-2f)/12\pi$. Here $f$ is the number of quark flavors and $t=\ln(Q^2/\Lambda^2)$. In the usual hadronic case there are four such functions corresponding to the parton transitions $q\to qg$, $q\to gq$, $g\to q\bar{q}$, and $g\to gg$. For the photon case there is an additional term[8] resulting from the transition $\gamma\to q\bar{q}$ which reflects the pointlike nature of the photon-quark coupling. Allowing for this extra term yields the result given in Ref. 8:

$$\begin{aligned}
\frac{dG_{q_i/\gamma}}{dt}(x,t) &= \int dy\, dz\, \delta(x-yz)\left\{\frac{\alpha_s(t)}{2\pi}\left[P_{qq}(y)G_{q_i/\gamma}(z,t)+P_{qg}(y)G_{g/\gamma}(z,t)\right]+\frac{\alpha Q_i^{\,2}}{2\pi}P_{q\gamma}(y)G_{\gamma/\gamma}(z,t)\right\},\\
\frac{dG_{g/\gamma}}{dt}(x,t) &= \frac{\alpha_s(t)}{2\pi}\int dy\, dz\, \delta(x-yz)\left[P_{gq}(y)\sum_{i=1}^{2f}G_{q_i/\gamma}(z,t)+P_{gg}(y)G_{g/\gamma}(z,t)\right],
\end{aligned} \tag{2}$$

where $Q_i$ denotes the fractional charge of the $i$th quark. Now, to lowest order in $\alpha$, $G_{\gamma/\gamma}(z,t)$ is just given by $\delta(1-z)$ so that for the new term both the $y$ and $z$ integrations can be performed trivially. The function $P_{q\gamma}(y)$ is the same as $P_{qg}(y)$ apart from a color factor. It is important to realize that in calculating the probability functions $P_{ij}(y)$ in Ref. 9 a sum over final colors and an average over initial colors was performed. Thus, the parton distribution functions in Eqs. (2) have been summed over colors. The color factor of $\frac{1}{2}$ in $P_{qg}(y)$ must be removed and replaced by a factor of 3 giving

$$P_{q\gamma}(y)=3[y+(1-y)^2]. \tag{3}$$

This factor of 3 was not included in Eq. (26) of Ref. 8.

The coupled set of equations in Eq. (2) can be easily solved by first taking moments. Defining

$$G^n_{a/A}(t)=\int dx\, x^{n-1}G_{a/A}(x,t),$$

$$A^n_{ij}=\frac{1}{2\pi b}\int dx\, x^{n-1}P_{ij}(x),$$

$$a^n=\frac{\alpha}{2\pi}\int dx\, x^{n-1}P_{q\gamma}(x)$$

yields the following equations for the moments:

$$\begin{aligned}
\frac{dG^n_{q_i/\gamma}}{dt}(t) &= Q_i^{\,2}a^n+\frac{1}{t}\left[A^n_{qq}G^n_{q_i/\gamma}(t)+A^n_{qg}G^n_{g/\gamma}(t)\right],\\
\frac{dG^n_{g/\gamma}}{dt}(t) &= \frac{1}{t}\left[A^n_{gq}\sum_{i=1}^{2f}G^n_{q_i/\gamma}(t)+A^n_{gg}G^n_{g/\gamma}(t)\right].
\end{aligned} \tag{4}$$

In the leading-logarithm solution each of the moments is proportional to $t$. Taking this into account yields a set of equations[8] which can be solved algebraically for the three independent distributions corresponding to charge $\frac{2}{3}$ and $\frac{1}{3}$ quarks and the gluons. The results for the moments are

$$\begin{aligned}
G^n_{q_i/\gamma}(t) &= a_n\left(\frac{Q_i^{\,2}-\frac{5}{18}}{1-A^n_{qq}}+\frac{5}{18}\frac{1-A^n_{gg}}{F_n}\right)t,\\
G^n_{g/\gamma}(t) &= \tfrac{20}{9}\,a_n\frac{A^n_{gq}}{F_n}t,
\end{aligned} \tag{5}$$

where $F_n=1-A^n_{qq}-A^n_{gg}+A^n_{qq}A^n_{gg}-2fA^n_{qg}A^n_{gq}$. This result for the moments of the gluon distribution agrees with the result of Ref. 7 if the latter is

multiplied by 8 to take the color sum into account. However, it is a factor of 3 larger than the corresponding result in Ref. 8 as a result of the factor of 3 appearing in Eq. (3).

The expressions for the moments in Eq. (5) have been used, together with the approximation technique of Yndurain,[10] to obtain the $x$-dependent parton distribution functions for the photon. The results are in agreement with those shown in Fig. 4 of Ref. 7.

For the nucleon case the input quark distributions at $Q_0^2 = 4$ (GeV/$c$)$^2$ were taken from Ref. 11, while the input gluon distribution was taken as

$$xG_{g/p}(x, Q_0^2) = 0.892(1+9x)(1-x)^4 .$$

This has the same form as that used in Ref. 12, but the normalization has been altered so as to satisfy the momentum sum rule when used with the quark distributions specified above. As in previous analyses the strong running coupling constant has been calculated for four quark flavors and the scale parameter $\Lambda$ has been taken to be 0.4 GeV/$c$. The $Q^2$ definition of Ref. 12 has been used, $Q^2 = 2stu/(s^2+t^2+u^2)$, where $s$, $t$, and $u$ are the Mandelstam variables for the hard-scattering subprocesses.

### B. Subprocess expressions

The subprocesses contributing to the four-jet event topology are the same ones that occur in hardon-hadron collisions, i.e., $qq \to qq$, $qg \to qg$, $gg \to gg$, $q\bar{q} \to gg$, $gg \to q\bar{q}$, and related ones involving antiquarks. The expressions for these are well known and may be found in Ref. 13.

The direct photon-quark coupling introduces two new subprocesses which are $\gamma q \to gq$ and $\gamma g \to q\bar{q}$. The cross-section expressions are given by

$$\frac{d\sigma}{dt}(\gamma q_i \to g q_i) = -\frac{\pi\alpha\alpha_s Q_i^2}{s^2}\frac{8}{3}\left(\frac{u}{s}+\frac{s}{u}\right), \tag{6}$$

and

$$\frac{d\sigma}{dt}(\gamma g \to q_i\bar{q}_i) = \frac{\pi\alpha\alpha_s Q_i^2}{s^2}\left(\frac{u}{t}+\frac{t}{u}\right). \tag{7}$$

The first of these, Eq. (6), has been discussed as a source of gluon jets in Ref. 14.

### C. Cross-section expressions

In this calculation the usual practice of using massless kinematics for the produced partons will be followed. The generalization to massive jets has been presented in Ref. 15 and will be discussed in Sec. IV. With the approximation that the initial partons are collinear in the overall center-of-mass system the cross section for high-$p_T$ jets is given by

$$E\frac{d^3\sigma}{dp^3}(\gamma + p \to \text{jet} + X) = \frac{1}{\pi}\sum_{ab}\int dx_a\, dx_b G_{a/\gamma}(x_a, Q^2) G_{b/p}(x_b, Q^2) \times \hat{s}\frac{d\sigma}{d\hat{t}}(a+b \to \text{jet}+X)\delta(\hat{s}+\hat{t}+\hat{u}). \tag{8}$$

for the four-jet event topology. Here a caret is used to denote the Mandelstam variables for the hard-scattering subprocess. For the three-jet topology the photon parton distribution function is replaced by a $\delta$ function. Thus, the four- and three-jet cross sections involve one and zero integrations, respectively. The resulting expression for the four-jet cross section is

$$E\frac{d^3\sigma}{dp^3}(\gamma + p \to \text{jet} + X) = \frac{1}{\pi}\sum_{ab}\int dx_a G_{a/\gamma}(x_a, Q^2) G_{b/p}(x_b, Q^2) \times \frac{2x_a x_b}{2x_a - x_T e^y}\frac{d\sigma}{d\hat{t}}(a+b \to \text{jet}+X), \tag{9}$$

where

$$x_b = \frac{x_a x_T e^{-y}}{2x_a - x_T e^y}$$

and $x_T = 2p_T/\sqrt{s}$. For the three-jet cross section

$$E\frac{d^3\sigma}{dp^3}(\gamma + p \to \text{jet} + X) = \frac{1}{\pi}\sum_{b} x_b G_{b/p}(x_b, Q^2)\frac{2}{2 - x_T e^y}\frac{d\sigma}{d\hat{t}}(\gamma + b \to \text{jet}+X) \tag{10}$$

with

$$x_b = \frac{x_T e^{-y}}{2 - x_T e^y}.$$

In Eqs. (9) and (10) the center-of-mass rapidity of the detected jet is denoted by $y$ which, for a massless jet, is related to the center-of-mass scattering angle $\theta$ by $y = \ln(\cot\theta/2)$.

In the next section, results for both single-jet and two-jet cross sections will be presented. As discussed in Ref. 16 two-jet cross sections can provide useful information in addition to that which can be obtained from single-jet measurements. Denoting the two-jet rapidities by $y_1$ and $y_2$, the two-jet invariant cross section for the four-jet event topology takes the form

$$\frac{d\sigma}{dy_1 dy_2 dp_T^2}(\gamma + p \to j_1 + j_2 + X) = \sum_{ab} x_a G_{a/\gamma}(x_a, Q^2) x_b G_{b/p}(x_b, Q^2) \times \frac{d\sigma}{d\hat{t}}(a+b \to j_1 + j_2 + X) \tag{11}$$

with

$$x_{a,b} = \tfrac{1}{2} x_T (\cosh y_1 + \cosh y_2 \pm \sinh y_1 \pm \sinh y_2) .$$

The corresponding quantity for the three-jet topology is not well defined since it contains a $\delta$ function. This occurs because for these subprocesses $y_2$ is determined by momentum conservation once $y_1$, $p_T$, and $s$ are specified. The two-jet cross section can be formally written in this case as

$$\frac{d\sigma}{dy_1 dy_2 dp_T^2}(\gamma + p \to j_1 + j_2 + X) = 2 \sum_b x_b G_{b/p}(x_b, Q^2) \frac{d\sigma}{d\hat{t}}(\gamma + b \to j_1 + j_2 + X) \times \delta(2 - x_T e^{y_1} - x_T e^{y_2}) . \quad (12)$$

Of course, in any experiment the $\delta$ function will be smeared out by the resolution in $y_2$ so that experimentally one measures

$$\frac{d\sigma(\Delta y_2)}{dy_1 dy_2 dp_T^2} = \frac{1}{\Delta y_2} \int dy_2 \frac{d\sigma}{dy_1 dy_2 dp_T^2} = \frac{1}{\Delta y_2} \sum_b x_b G_{b/p}(x_b, Q^2) \frac{2}{2 - x_T e^{y_1}} \times \frac{d\sigma}{d\hat{t}}(\gamma + b \to j_1 + j_2 + X) . \quad (13)$$

Here $x_b$ and $y_2$ are given by

$$x_b = \frac{x_T e^{-y_1}}{2 - x_T e^{y_1}}$$

and

$$y_2 = \ln\left(\frac{2}{x_T} - e^{y_1}\right) .$$

The two-jet results presented in the next section have been calculated using Eq. (13) with $\Delta y_2 = 0.1$. The results can be scaled simply if another choice for $\Delta y_2$ is desired.

## III. PREDICTIONS

### A. Single-jet triggers

To initiate the discussion of the QCD predictions for high-$p_T$ jet photoproduction, consider the case where a single jet is used as the trigger. The prediction for the inclusive invariant jet cross section at $\sqrt{s} = 19.4$ GeV and $y = 0$ is shown in Fig. 1. Also shown are the individual contributions from the three-jet and four-jet subprocesses. The latter contributions are labeled by the three possible final states $qq$, $qg$, and $gg$, where both quark and antiquark contributions are labeled as $q$. In the lower portion of the $p_T$ scale the four-jet contributions dominate. The relative importance of the various subprocesses is the same as in the purely hadronic processes—$gq \to gq$ dominates, followed by $gg \to gg$ and $qq \to qq$. As the value of $p_T$ is increased the three-jet subprocesses start to become more important and after $p_T \simeq 5\,\mathrm{GeV}/c$ the dominant contribution is from $\gamma q \to gq$. The flatter $p_T$ slope of the three-jet processes is a reflection of the fact that all of the photon's energy contributes to the hard scattering. The contributions from the four-jet processes fall off somewhat faster with increasing $p_T$ as a result of the decrease of the photon's parton distribution functions. Even so, this falloff is more gradual than in the purely hadronic case. It should be emphasized that as a result of the more gradual $p_T$ dependence the photoproduction cross section at $p_T \gtrsim 6\,\mathrm{GeV}/c$ is predicted to exceed the corresponding cross sections for pion or proton beams.

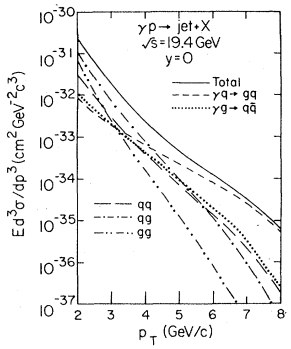


FIG. 1. Prediction for the invariant jet cross section at $\sqrt{s} = 19.4$ GeV and $y = 0$ together with the contributions of the various subprocesses. The labels $qq$, $qg$, and $gg$ refer to the possible final states for the parton-parton scattering subprocesses.

In the absence of scale-violating effects, the cross section given by Eq. (8) predicts a behavior at fixed $x_T$ and $\theta$ of

$$Ed^3\sigma/dp^3 = A p_T^{-n} f(x_T, \theta) , \quad (14)$$

where $n = 4$ for the QCD subprocesses considered here. This behavior is modified by the $Q^2$ dependences in the distribution functions and the strong running coupling constant. There is, however, a cancellation between the $Q^2$ dependence in the photon distribution function and $\alpha_s(Q^2)$ such that $\alpha_s(Q^2) G_{i/\gamma}(x, Q^2)$ scales for both quarks and gluons. Thus, for both the three- and four-jet processes the only $Q^2$ dependence comes from one power of $\alpha_s(Q^2)$ and from the scale-violating nucleon

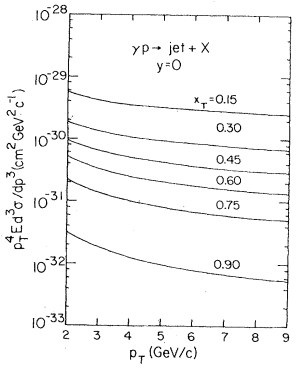


FIG. 2. Predictions for the invariant jet cross section weighted by $p_T^4$ at fixed $x_T$ with $y=0$.

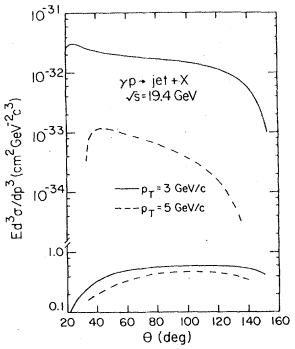


FIG. 3. Predictions for the angular dependence of the invariant jet cross section at $\sqrt{s}=19.4$ GeV with $p_T=3$ GeV/$c$ (solid line) and 5 GeV/$c$ (dashed line). Also shown (in the lower part of the figure) are the predictions for the gluon-jet trigger ratio $R_g$ defined by Eq. (15).

distribution functions. There is only a slight modification of the naive scaling prediction with $n$ being shifted from 4 to about 4.5 at low $x_T$ and about 5 at high $x_T$. This is illustrated in Fig. 2 where the jet cross section has been weighted by $p_T^4$. As expected, there remains only a slight decrease with $p_T$ at fixed $x_T$ and $\theta$. A discussion of various factors which might modify these predictions is given in Sec. IV.

The angular dependence of the jet photoproduction cross section is markedly different from the hadronic case. With a hadron beam and target the cross section falls off smoothly as the center-of-mass angle goes towards either 0° or 180° since these regions correspond to $x_a$ or $x_b$ being large, respectively, and hence, the beam or target distribution functions decrease strongly. The photoproduction predictions for two $p_T$ values at $\sqrt{s}=19.4$ GeV are shown in Fig. 3. A smooth decrease is seen at large angles as in the hadronic case. This region corresponds to large $x$ for the target and so the decrease is controlled by the proton distribution functions. At smaller angles, however, the situation is quite different. Here the shape is controlled by the much flatter large-$x$ behavior of the photon quark distribution functions and the cross section actually rises at sufficiently small angles. This forward-backward asymmetry is a striking effect which should stand out clearly. Its observation would provide important confirmation of the expected form of these functions. It should be pointed out, however, that the flat shape of $G_{q/\gamma}(x, Q^2)$ is due primarily to the structure of the $\gamma \to q\bar{q}$ vertex and, as a result, the observation of this asymmetry is not a direct test of QCD.

Also shown in Fig. 3 are predictions for the angular dependence of the ratio $R_g$, defined by

$$R_g = n_g/(n_q+n_g)\,, \tag{15}$$

where $n_q$ ($n_g$) is the number of quark- (gluon) jet triggers. At small angles, quark jets dominate the single-jet cross section. This happens, in part, because this region corresponds to large $x$ for the photon distribution functions so that quark-induced subprocesses dominate. Thus, this is a reflection of the forward peaking discussed above and shown also in Fig. 3. At larger angles $R_g$ increases to about 50% reflecting the dominance of the two subprocesses $gq \to gq$ and $\gamma q \to gq$. It would be interesting to compare the properties of jets produced at low angles with those produced near $\theta = 90°$ since the former should be dominated by quark jets while the latter should have a roughly equal mixture of both quark and gluon jets.

### B. Two-jet triggers

Triggers which are based on the simultaneous detection of two high-$p_T$ jets provide additional information not obtainable with a single-jet trigger mode of operation.[4] For example, the momentum imbalance between the two jets yields information concerning the transverse-momentum distributions of the colliding partons. In addition, it is possible to define a two-jet cross section which is relatively insensitive to the uncertainties associated with the treatment of the initial parton-transverse-momentum smearing. This has been shown[16] to be the case for the two-jet cross

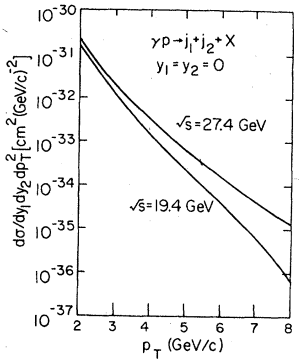


FIG. 4. Predictions for the two-jet cross section at $y_1 = y_2 = 0$ and $\sqrt{s} = 19.4$ and 27.4 GeV.

section given by Eq. (11).

Predictions for the two-jet cross section at $\sqrt{s} = 19.4$ and 27.4 GeV are shown in Fig. 4 for $y_1 = y_2 = 0$. An interesting feature of the two-jet cross section is that unless $y_2$ and $y_1$ are related by

$$y_2 = \ln\left(\frac{2}{x_T} - e^{y_1}\right), \tag{16}$$

only the four-jet processes will contribute to the cross section. This point is illustrated in Fig. 5 which shows away-side rapidity distributions for $y_1 = 0$ and $\sqrt{s} = 19.4$ GeV. The three-jet processes contribute at the kinematic limits designated by the arrows. The three-jet processes have been calculated according to Eq. (13) so that the area

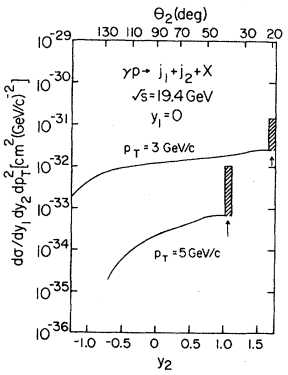


FIG. 5. Predictions for the away-side jet rapidity distribution at $\sqrt{s} = 19.4$ GeV with $y_1 = 0$. The arrows show the kinematic limit at each value of $p_T$ and the shaded rectangles show the contributions of the three-jet processes. For convenience, the upper scale shows the away-side jet center-of-mass scattering angle $\theta_2$.

contained in each shaded rectangle represents the total three-jet contribution. This feature means that with the use of a sufficiently sophisticated detector the three- and four-jet contributions may be separated. Furthermore, at large values of $x_T$, e.g., $x_T > 0.4$, the $\gamma q \to gq$ subprocesses dominates over the $\gamma g \to q\bar{q}$ subprocesses. Thus, a separate measurement of the "QCD Compton effect"[14] should be possible. This measurement should provide an interesting test of QCD since it depends only on the well measured nucleon quark distribution functions and on the QCD-predicted subprocess expression. There is no uncertainty stemming from initial gluons and the parton $k_T$ effects are limited by the kinematics employed in the two-jet trigger.

In a recent publication[17] it has been pointed out that it will be difficult to measure the QCD Compton effect with a single-arm trigger because of the competition from the four-jet events and the $\gamma g \to q\bar{q}$ subprocesses. This conclusion is consistent with the results of the calculations presented here. However, as discussed above, a double-arm trigger can be used to separate the contributions of the three- and four-jet subprocesses by taking advantage of their kinematic differences. This separation does not require the identification of quark or gluon jets. Therefore, it seems to be possible to measure the QCD Compton effect without such jet identification. Indeed, clearly separating out this subprocess may help in the search for identifying characteristics of quark and gluon jets.

## IV. BACKGROUNDS AND SOURCES OF THEORETICAL UNCERTAINTY

The cross-section predictions presented in the previous section result from subprocesses in which the photon either interacts with quarks in a pointlike fashion or serves as a source of quarks and gluons as a result of the $\gamma \to q\bar{q}$ transition in conjunction with the QCD evolution equations. In addition, it is well known that the photon can interact as if it were a vector meson. It is easy to predict the background coming from this type of interaction using the vector-dominance model. Assuming that the photon interacts in the same manner as a $\rho$ meson gives the relation

$$\sigma(\gamma p \to \text{jet} + X) \simeq \left(\frac{4\pi\alpha}{f_V^2}\right)\sigma(\rho^0 p \to \text{jet} + X)$$
$$\simeq \left(\frac{4\pi\alpha}{f_V^2}\right)\sigma(\pi^0 p \to \text{jet} + X), \tag{17}$$

where the last line follows from the assumption that the parton distributions in a $\pi^0$ are the same as for a $\rho^0$. For the $\rho$-$\gamma$ coupling the value $f_V^2/4\pi = 2.2$[18] has been used. Contributions from $\omega$

and $\phi$ terms are about an order of magnitude smaller and have been neglected here.

Data from the Fermilab experiment E-260 (Ref. 19) show that the $\pi^+$ and $\pi^-$ induced jet cross sections are nearly equal. The assumption that the $\pi^0$ induced cross section is given by the average of the $\pi^+$ and $\pi^-$ induced cross sections together with Eq. (17) yields the vector-dominance prediction shown in Fig. 6. Clearly, the vector-dominance background is not a problem in the region above $p_T = 3$ GeV/$c$. This occurs primarily because of the stronger decrease with $p_T$ which is exhibited by the purely hadronic processes which in turn is a result of the faster decrease with increasing $x$ of the hadronic parton distribution functions as compared with those of the photon.

A more difficult problem concerns the question of parton-transverse-momentum ($k_T$) effects. As a result of the steeply falling $p_T$ spectrum the single-jet trigger will preferentially select those events in which the parton-parton center-of-mass system is moving towards the detector. This results in a smearing of the $p_T$ distribution which can lead to a large enhancement of the cross section. However, the precise magnitude of the effect depends crucially on the treatment of the initial partons. If on-shell kinematics is used then a large cross-section enhancement results[12,16]; but only a modest effect is observed if the partons are treated as being off-shell.[20] In hadron-hadron interactions it is argued[12] that there are two components contributing to the parton-$k_T$ effects. First, there is an intrinsic or primordial component resulting from confining the partons, and then there are contributions from higher-order, e.g., $2 \to 3$, subprocesses. Now for photon-induced reactions the only intrinsic term will be that of the target proton. Thus, the effect of the parton $k_T$ smearing should be somewhat reduced as compared to the purely hadronic case. The exact degree of the reduction depends on the relative importance of the intrinsic and higher-order terms.

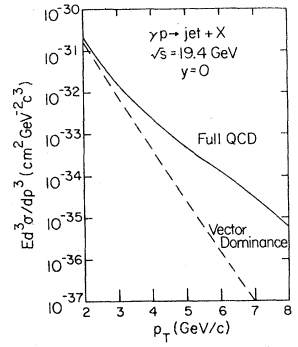


FIG. 6. Comparison at $\sqrt{s} = 19.4$ GeV and $y = 0$ of the full QCD prediction and the vector-dominance background prediction discussed in the text.

As an aside, notice that the vector-dominance prediction shown in Fig. 6 was obtained using the observed jet cross section[19] and, as a result, is independent of the question of parton-$k_T$ smearing. If the theoretical QCD predictions are increased by including such effects then this background becomes even less important.

The parton-$k_T$ smearing most strongly affects the lower-$p_T$ region and decreases in importance as the $p_T$ is increased. This is a specific example of the more general phenomenon that in the region where $p_T$ is large but $x_T$ is small there are at least two large momentum scales and the leading-logarithmic calculations may not be reliable. The QCD predictions presented here are expected to be most reliable in the region where the choice of the large momentum scale is unambiguous, i.e., $x_T$ near 1.

Because the parton $k_T$ effects are $p_T$ dependent, the scaling behavior shown in Fig. 2 may be modified. The exponent $n$ in hadron reactions is typically increased by about two units. For the photoproduction case a somewhat smaller effect might be expected as discussed above so that $n \simeq 6$ may be observed. This, however, would be a transient effect which would vanish with increasing $p_T$.

The role of the parton-$k_T$ smearing can be investigated using a double-arm trigger as mentioned previously. The observed transverse-momentum imbalance between the two high-$p_T$ jets is a reflection of the effects due to the intrinsic $k_T$ and/or more complicated higher-order terms such as $2 \to 3$ subprocesses. Also, the two-jet cross section should be relatively insensitive to the parton $k_T$ smearing effects.[16]

A $p_T^{-6}$ dependence can also result from the presence of more complicated subprocesses such as those found in the constituent-interchange model (CIM), e.g., $\gamma M \to q\bar{q}$ and $\gamma q \to Mq$ where $M$ is a meson.[21] However, it is not expected that CIM diagrams will make a large contribution to jet processes relative to the QCD subprocesses because the latter are not subject to the trigger bias suppression which occurs in single-particle triggers. Thus, the ratio of CIM/QCD contributions should be much smaller for jet triggers than for single-particle triggers. Indeed, there is some experimental evidence[4] from hadron-hadron jet reactions that subprocesses such as $Mq \to Mq$ are not playing a large role since both the toward and,

away-side jets are observed to have very similar properties. For this reason the possible CIM contributions have not been included here.

Another source of uncertainty in jet cross-section calculations has been the question of whether the jet energy or jet momentum should be used when comparing theory and experiment. A recent calculation[15] in which jet masses appeared explicitly showed that the inclusion of jet masses reduced the cross section at $\sqrt{s}=19.4$ GeV in $pp$ collisions by a factor of 2 (5) for the $ud \to ud$ ($gg \to gg$) subprocesses when the results were plotted versus the jet $p_T$. Most of this effect resulted from the shift to slightly higher values of $x_a$ and $x_b$ when massive jets were produced thus causing a reduction in the parton distribution functions. The suppression will be smaller in the photoproduction case because of the slower variation with $x$ of the photon parton distribution functions. Therefore, the neglect of the jet-mass effects in this analysis will not introduce too large a degree of uncertainty in the predictions.

The cross-section predictions presented here should provide a reliable guide for designing future experiments. The two main sources of theoretical uncertainty are parton $k_T$ smearing and jet-mass effects. Both should be smaller than in the purely hadronic case, and, to some extent, they offset each other since the former would increase the predictions while the latter would decrease them. Based on a comparison with similar effects in hadron-hadron collisions, it appears that the predictions given here can be treated as conservative lower limits for the jet photoproduction cross sections.

## V. SUMMARY AND CONCLUSIONS

The study of high-$p_T$ jet photoproduction can be a means of obtaining new information relevant to the understanding of the underlying parton scattering processes. New subprocesses not present in purely hadronic reactions contribute here and can be separated on a purely kinematic basis if a detector with sufficiently large acceptance is used. It may also be possible to determine some characteristics of the photon parton distribution functions. By studying the cross section in different kinematic regions it is possible to vary the percentage of gluon versus quark jets. Thus, it may be possible to discern differences between the two types of jets.

Photons are relatively more efficient at producing high-$p_T$ jets than are hadrons. The predicted cross sections for $p_T > 6$ GeV/$c$ exceed those for hadron beams even though the coupling has been reduced by a factor of $\alpha$. Therefore, high-$p_T$ jet photoproduction experiments appear to be both practical and interesting.

*Note added in proof.* The factor-of-three discrepancy in Ref. 8 discussed in Sec. II has been corrected and an additional clarifying discussion has been given in Ref. 22.

## ACKNOWLEDGMENT

This work was supported in part by the U. S. Department of Energy.

[1] R. D. Field, in *Proceedings of the 19th International Conference on High Energy Physics, Tokyo, 1978*, edited by S. Homma, M. Kawaguchi, and H. Miyazawa (Physical Society of Japan, Tokyo, 1979), p. 743.
[2] J. F. Owens in, *High Energy Physics in the Einstein Centennial Year*, proceedings of Orbis Scientiae, Coral Gables, 1979, edited by A. Perlmutter, F. Krausz, and L. Scott (Plenum, New York, 1979), p. 347.
[3] M. Tannenbaum, Rockefeller University Report No. COO-2232A-79, 1979, to be published in the Proceedings of the XIVth Rencontre de Moriond.
[4] W. Selove, University of Pennsylvania Report No. UPR-70E, 1979, to be published in the Proceedings of the XIVth Rencontre de Moriond.
[5] M. Dris *et al.*, Phys. Rev. D 19, 1361 (1979).
[6] E. Witten, Nucl. Phys. B120, 189 (1977).
[7] C. H. Llewllyn Smith, Phys. Lett. 79B, 83 (1978).
[8] R. J. DeWitt *et al.*, Phys. Rev. D 19, 2046 (1979).
[9] G. Altarelli and G. Parisi, Nucl. Phys. B126, 298 (1977).
[10] F. J. Yndurain, Phys. Lett. 74B, 68 (1978).
[11] J. F. Owens and J. D. Kimel, Phys. Rev. D 18, 3313 (1978).
[12] R. P. Feynman, R. D. Field, and G. C. Fox, Phys. Rev. D 18, 3320 (1978).
[13] B. L. Combridge, J. Kripfganz, and J. Ranft, Phys. Lett. 70B, 234 (1977); R. Cutler and D. Sivers, Phys. Rev. D 17, 196 (1978); J. F. Owens, E. Reya, and M. Glück, *ibid.* 18, 1501 (1978).
[14] H. Fritzsch and P. Minkowski, Phys. Lett. 69B, 316 (1977).
[15] J. F. Owens, Phys. Rev. D (to be published).
[16] J. F. Owens, Phys. Rev. D 20, 221 (1979); Report No. FSU-HEP-790427, 1979, to be published in the Proceedings of the XIVth Rencontre de Moriond.
[17] Tu Tung-sheng, CERN Report No. Ref. TH. 2690, 1979 (unpublished).
[18] H. Pilkuhn *et al.*, Nucl. Phys. B65, 460 (1973).
[19] C. Bromberg *et al.*, Caltech Report No. CALT-68-724, 1979 (unpublished).
[20] W. E. Caswell, R. R. Horgan, and S. J. Brodsky, Phys. Rev. D 18, 2415 (1978); R. R. Horgan and P. N. Scharbach, Phys. Lett. 81B, 215 (1979).
[21] R. Rückl, S. J. Brodsky, and J. F. Gunion, Phys. Rev. D 18, 2469 (1978).
[22] R. J. Dewitt *et al.*, Phys. Rev. D 20, 1751(E) (1979).